Journal of Asian Concrete Federation

journal homepage: https://jacf.sfulib3.publicknowledgeproject.org/index.php/jacf

Recent progress in carbon mineralization of aerated concrete and steel slag products with insights into aluminosilicate glass reactivity

Sen Zhang[1,2,3], Yang Yu [1,2,3], Cuifang Lu [1,2,3], Mohammed Ali M. Rihan [1,2,3], Xin Wang [1,2,3], Xiang Hu [1,2,3,*]

[1] *College of Civil Engineering, Hunan University, Changsha 410082, P. R. China*
[2] *Key Laboratory for Green & Advanced Civil Engineering Materials and Application Technology of Hunan Province, Changsha 410082, P. R. China*
[3] *Key Laboratory of Building Safety and Energy Efficiency of the Ministry of Education, Hunan University, Changsha 410082, P. R. China*

A B S T R A C T

Carbon mineralization has emerged as a promising strategy for mitigating CO_2 emissions in the construction industry by permanently converting CO_2 into thermodynamically stable carbonate phases. This review provides a comprehensive overview of recent advances in the carbonation of CO_2-aerated concrete, carbonated steel slag products, and aluminosilicate-rich glassy materials. For CO_2-aerated concrete, carbonation integrated with foaming or curing processes significantly enhances early-age strength, refines the pore structure, improves thermal insulation, and increases long-term carbon sequestration capacity. Regarding steel slag, the direct production of fully carbonated blocks and bricks is identified as a more effective utilization pathway than employing carbonated steel slag as a supplementary cementitious material or aggregate, owing to its superior dimensional stability, mechanical performance, and CO_2 sequestration potential. For aluminosilicate glassy phases, aluminum inhibits carbonation by reducing Ca^{2+} dissolution and suppressing $CaCO_3$ nucleation, whereas mechanical activation effectively disrupts the glass network, accelerates ion release, and promotes carbonation reactions. Future research should prioritize the development of standardized carbon-accounting methodologies, scalable and energy-efficient carbonation technologies, and robust durability assessment frameworks to facilitate the widespread implementation of carbon-negative construction materials.

Keywords: Carbon mineralization, CO_2-aerated concrete, carbonated steel slag, carbonated aggregates, aluminosilicate glasses

1. Introduction

The construction industry is recognized as one of the largest contributors to anthropogenic carbon dioxide (CO_2) emissions, making the development of effective decarbonization strategies a global priority. Among the available approaches, carbon capture, utilization, and storage (CCUS) has gained widespread attention as a key pathway for mitigating industrial CO_2 emissions [1, 2]. Within the CCUS framework, carbon mineralization, also referred to as mineral carbonation or CO_2 mineralization, has emerged as a particularly promising technology because it permanently immobilizes gaseous CO_2 by converting it into thermodynamically stable carbonate minerals. This process provides long-term, leakage-resistant carbon sequestration while simultaneously producing value-added carbonate-based materials with potential industrial applications [3-7]. The fundamental mechanism of carbon mineralization involves the reaction of CO_2 with calcium- and magnesium-bearing alkaline earth phases to form stable carbonate minerals. The following generalized reaction can represent this process:

$$(Ca,Mg)O + CO_2 \rightarrow (Ca,Mg)CO_3$$

Building materials constitute an especially compelling carrier for this reaction for three reasons. First, their enormous production volume offers a correspondingly large potential CO_2 sink [5, 6, 8, 9]. Second, the feedstocks involved Portland cement, hydration products, and Ca/Mg-rich industrial by-products such as steel slag, blast-furnace slag, and fly ash are inherently reactive toward CO_2 [10-13]. Third, the in situ-formed carbonate products can fill pores, densify the microstructure, and improve mechanical strength and durability, thereby transforming CO_2 from a waste gas into a functional component of the material

* Corresponding author: Xiang Hu (xianghu@hnu.edu.cn)

DOI http://dx.doi.org/10.18702/acf.2026.12.1.???

Received: 24-Jun-2026; Revised: 19-Aug-2026; Accepted: 03-Sep-2026; Published online: 17-November-2026

ISSN 2465-7964, eISSN 2465-7972. Copyright © Asian Concrete Federation, All rights reserved.

[14-16]. In this way, carbon mineralization couples emission reduction with resource recovery and solid-waste valorization, aligning closely with the circular economy and "all-solid-waste cementitious material" objectives now embodied in national industrial-green-development policies.

Despite this promise, the practical implementation of carbon mineralization in building materials is constrained by several fundamental bottlenecks [17-19]. In conventional dense concrete, the rapid formation of a $CaCO_3$ layer at the surface hinders the further inward diffusion of CO_2, confining carbonation to a shallow depth [20-22]. Steel slag, although rich in carbonatable Ca and Mg, suffers from poor hydraulic activity and severe volume instability caused by free CaO and MgO, which restricts its large-scale, high-value reuse [23-28]. Moreover, the aluminosilicate glassy phases that dominate many industrial residues exhibit intrinsically low carbonation reactivity, and the role of network-modifying elements particularly Al in suppressing Ca^{2+} release and $CaCO_3$ nucleation remains incompletely understood [29-33]. Overcoming these limitations is essential before carbon-mineralized building products can be deployed at scale.

Motivated by these challenges, this review summarizes recent progress in applying carbon mineralization technology to the preparation of building materials and products along three representative directions. The first concerns CO_2-aerated concrete, in which CO_2 is introduced either as a foaming medium or as a curing agent to exploit the mass-transfer advantages of a porous structure, and examines its preparation routes, mineralization mechanisms, macroscopic performance and carbon-sequestration behavior. The second addresses the carbon mineralization of steel slag, critically comparing its use as a supplementary cementitious material, as an artificial aggregate, and as pure carbonated steel-slag products, with emphasis on which route best reconciles volume stabilization, mechanical adequacy and maximal CO_2 uptake. The third focuses on the influence of Al in aluminosilicate glassy phases on carbonation, integrating evidence from synthetic glasses and real industrial wastes (slag and fly ash) at the atomic, nanoscale and reaction-interface levels, together with corresponding process-intensification strategies. These topics were selected because they address complementary limitations of carbon mineralization at different scales: CO_2 access in a porous building product, stabilization and bulk utilization of a reactive industrial residue, and the dissolution and precipitation kinetics of a less-reactive glass phase. Steel slag and other Ca-bearing wastes can also serve as constituents of aerated products, while the glass mechanisms help explain why apparently Ca-rich residues can respond differently to similar treatments. Together, the three topics connect transport, precursor reactivity, and product performance. The review is therefore a focused synthesis of these linked questions rather than an exhaustive survey of all mineralization applications. By connecting mechanisms, material performance and engineering practicality, this review aims to clarify the current state of the art and identify the key scientific and technological gaps that must be bridged to realize scalable, durable and genuinely carbon-negative building materials.

2. CO_2-aerated concrete

In conventional CO_2-cured concrete, rapid formation of a surface carbonate layer can restrict inward CO_2 transport and limit further carbonation. By contrast, in CO_2-aerated concrete, CO_2 is introduced directly into the internal pore network during the preparation process, allowing it to be uniformly distributed within the cementitious paste. This significantly reduces the CO_2 diffusion distance while increasing the gas–liquid–solid interfacial area available for carbonation reactions.

The preparation of CO_2-aerated concrete generally follows two approaches. The first employs CO_2 directly as the foaming medium, whereby the gas is incorporated into the slurry during mixing to generate a porous structure. The second involves carbonation curing after the aerated concrete has been formed. Despite their different processing routes, both approaches capitalize on the enhanced mass transport and reaction kinetics provided by the porous structure. As a result, they effectively overcome the fundamental limitation of conventional dense concrete namely, surface-localized carbonation with restricted CO_2 penetration into the interior.

2.1. Preparation route

2.1.1. CO_2-foamed concrete

In CO_2-foamed concrete, CO_2 replaces air as the primary gas phase within the foam bubbles, thereby enabling simultaneous lightweighting and in situ carbonation during the material preparation process. Rather than remaining in the pores as an inert gas, CO_2 readily dissolves in the pore solution adjacent to the bubble walls, where it reacts with Ca^{2+}, Mg^{2+}, and cement hydration products, resulting in a coupled mechanism of pore formation and carbon mineralization [34-38]. Nevertheless, CO_2-foamed concrete continues to face significant challenges related to foam stability. Because of the high solubility of CO_2 in water and the rapid acid base neutralization reaction between dissolved CO_2 and the highly alkaline cementitious slurry, the CO_2 foam dissipates quickly, causing bubble collapse, increasing the material density, and consequently diminishing the lightweighting effect. To overcome these limitations, two key strategies have been proposed. The first involves incorporating foam stabilizers to prolong the half-life of CO_2 foam and improve the uniformity of the bubble distribution. The second is the application of pre-carbonation treatment to regulate the initial alkalinity and rheological behavior of the slurry, thereby reducing the rate of CO_2 foam consumption during subsequent processing [37, 39]. For example, Fan et al. [38] employed sodium dodecyl sulfate (SDS) and ANS surfactants to optimize the pore structure of CO_2-capturing foamed concrete through the efficient utilization of CO_2 foam. Their approach reduced total porosity, refined the pore size distribution, and enhanced pore uniformity, as illustrated in Fig. 1. In general, these approaches are beneficial for balancing foam stability and strength development; however, their underlying mechanisms and limits of applicability still need to be systematically elucidated.

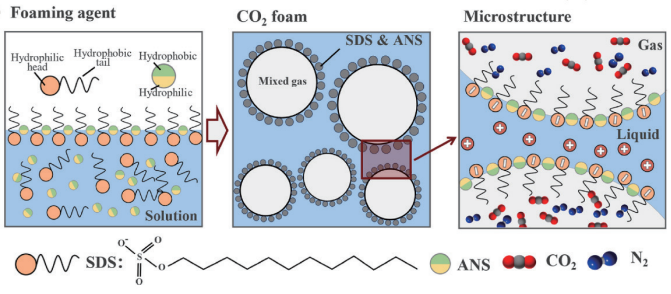


Fig.1. Foaming principle and foam stabilization mechanisms [38].

2.1.2. CO_2-cured aerated concrete

The key to CO_2-cured aerated concrete is to exploit the mass-transfer advantages arising from its high porosity and interconnected pore network, thereby facilitating the rapid inward diffusion of CO_2 at early ages and its mineralization reaction with reactive constituents. Consequently, the hardening mechanism gradually evolves from the conventional hydration-dominated mode to a synergistic hydration–carbonation hardening mode. Carbonation curing generally involves initial pre-curing to allow pore formation and sufficient early strength development, followed by exposing the formed aerated concrete to CO_2 in a controlled curing chamber. The main curing parameters include CO_2 pressure, temperature, relative humidity, and curing duration. In addition, the degree of pre-hydration should be carefully controlled, as insufficient pre-hydration may retain excessive moisture, while excessive pre-hydration can restrict CO_2 penetration[19]. In conventional AAC, siliceous raw materials such as fly ash, incineration bottom ash, and silica sand typically account for 60%–70% of the total mixture. While these components provide the structural framework and silica source, their carbonatable reactivity is relatively limited, making them insufficient to fully sustain efficient mineralization and the resulting strength gain. Therefore, in order to enhance reactivity under CO_2 curing conditions while also promoting the valorization of solid wastes, recent studies have explored the incorporation of Ca- rich or Mg-rich industrial residues as raw materials for aerated concrete [40-42]. Such materials generally exhibit relatively high potential hydration activity or carbonation reactivity, allowing the generation of more carbonate products during CO_2 curing, thereby improving matrix densification and enhancing early-age mechanical properties.

2.2. Mineralization mechanism

The role of CO_2 in aerated concrete should not be simply understood as an additional carbonation process, but rather be regarded as a continuous process composed of the coupling of pore formation, mass transfer, dissolution–migration, mineralization deposition, and performance enhancement. From the perspective of reaction mechanism, as shown in Fig. 2, the mineralization process in CO_2-foamed or CO_2-cured aerated concrete can generally be summarized into three successive stages: first, CO_2 is transported and diffuses through the pore structure; second, CO_2 dissolves in the pore solution and induces the migration and release of active ions such as Ca^{2+}; finally, the CO_3^{2-} reacts with Ca^{2+} to form carbonates, which then nucleate, grow, and deposit at specific interfaces [40, 43-45].

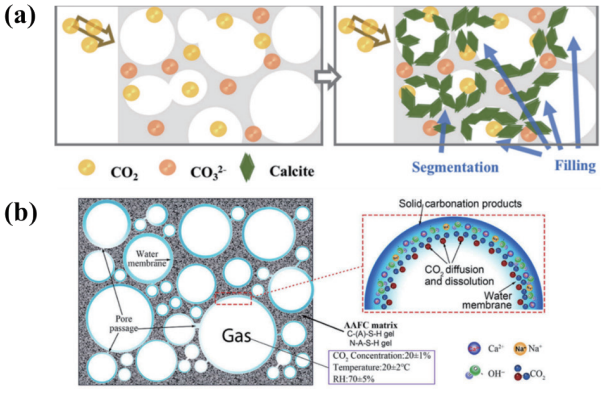


Fig. 2. Schematic diagram of CO_2 transmission and carbonation process: (a) CO_2-cured aerated concrete [46]; (b) CO_2-foamed concrete [45].

In terms of CO_2 diffusion, the transport pathways vary fundamentally depending on the method of CO_2 incorporation into the concrete. When CO_2 is applied as an external curing medium, gaseous CO_2 diffuses from the surface into the interior through interconnected pore channels, and its transport through the pore network is generally regarded as the rate-controlling step of the carbonation process. Specifically, millimeter-scale pores determine whether CO_2 can rapidly penetrate the interior of the material, whereas micrometer- and nanometer-scale pores govern CO_2 dissolution in the pore solution, ion transport, and the subsequent nucleation and deposition of carbonate phases [47]. It should be emphasized that, although high porosity facilitates CO_2 transport, it does not necessarily lead to enhanced material performance. Excessive porosity may improve CO_2 diffusion efficiency, but it can also compromise the matrix skeleton' s continuity and integrity. In addition, extensive carbonation may form carbonate layers around unhydrated cement particles, thereby hindering subsequent hydration and potentially affecting later-age strength development[46]. By contrast, when CO_2 is directly introduced into the slurry or concrete in the form of bubbles, its role is no longer manifested as conventional surface carbonation progressing from the exterior to the interior; instead, it becomes a localized mineralization process involving CO_2 storage within pores, localized dissolution at pore walls, and in situ $CaCO_3$ deposition at the interface. In this sense, CO_2 functions simultaneously as the pore-forming medium, the internal curing medium, and the mineralization reactant.

Subsequently, under liquid-phase conditions, CO_2 dissolves into the pore solution and, through dissociation reactions, establishes the carbonate system, while also inducing the gradual release of Ca^{2+} from unhydrated particles and pre-existing hydration products. Once the local ionic product exceeds the solubility product of $CaCO_3$, calcium carbonate preferentially nucleates, grows, and deposits at the gas-liquid-solid interface or in regions adjacent to the pore walls.

In contrast to external CO_2 curing, under which carbonate products tend to accumulate at the specimen surface, directly introduced CO_2 preferentially reacts in the vicinity of the pore walls. Consequently, the mineralization products are generally deposited along the inner pore wall surfaces rather than being uniformly distributed throughout the bulk matrix.

2.3. The effect of CO_2 incorporation on macroscopic properties

In terms of macroscopic performance, CO_2-aerated concrete generally exhibits synergistic improvements in lightweight properties, thermal insulation, early-age strength enhancement, and carbon sequestration. Whether introduced through external CO_2 curing or direct CO_2 entrainment, CO_2 not only alters the gaseous composition within the pore structure, but more importantly reconstructs the pore walls and local matrix through in situ mineralization, thereby markedly influencing the overall macroscopic properties of aerated concrete.

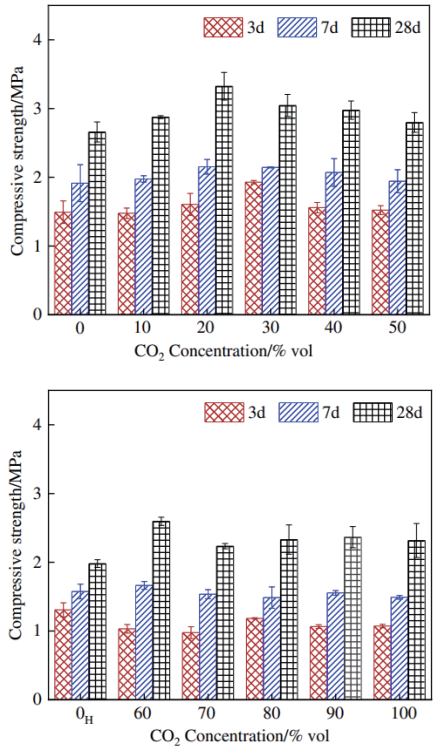
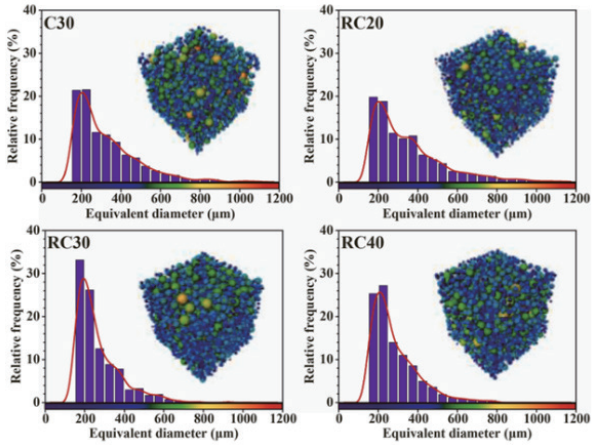


Fig. 3. Effect of CO_2 concentration on compressive strength [48].

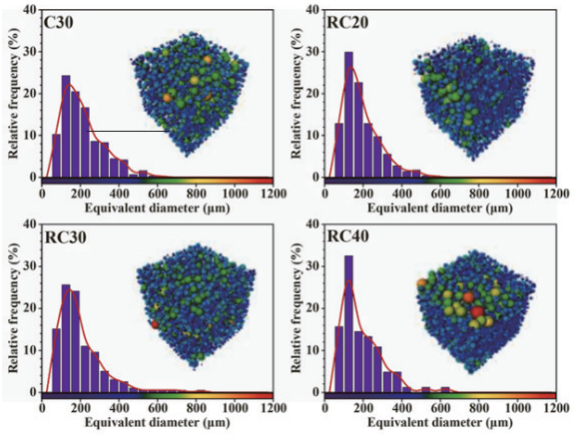
Regarding mechanical properties, one of the most prominent characteristics of CO_2-aerated concrete is its enhanced early-age strength. However, this strengthening effect does not increase monotonically with increasing CO_2 incorporation. The formation of carbonate phases on pore walls and particle surfaces enhances the early load-bearing capacity through pore filling, interparticle bridging, and matrix densification [24, 25, 37]. Nevertheless, these beneficial effects are typically observed only within an optimal carbonation range. When the degree of CO_2 incorporation becomes excessive, over-mineralization may induce local embrittlement, damage the pore-wall structure, and suppress subsequent hydration, thereby reducing the compressive strength, as shown in Fig. 3. Accordingly, the improvement in mechanical performance induced by CO_2 entrainment should be regarded as a controlled strengthening mechanism, whose effectiveness depends not on maximizing carbonation, but on achieving an appropriate balance among pore-structure stability, the degree of mineralization, and continued hydration.

With respect to dry density and lightweight characteristics, CO_2-aerated concrete maintains the fundamental advantages of conventional lightweight materials. In most studies, the dry density ranges from approximately 600 to 900 kg/m^3, satisfying the requirements for lightweight wall materials and thermal insulation applications. Moreover, compared with conventional foamed concrete, CO_2-aerated concrete generally exhibits a higher strength-to-density ratio. As shown in Fig. 4, the introduction of CO_2 does not compromise the lightweight nature of the material; instead, in situ mineralization along the pore walls enhances load-bearing efficiency at a given density, thereby providing a more favorable balance between low density and high mechanical strength [49, 50]. Despite these advantages, the use of steel slag as a cementitious component in CO_2-aerated concrete remains challenging. In several studies, steel slag has been employed as a partial or complete replacement for fly ash because of its high carbonation reactivity. However, its application is constrained by several inherent limitations. First, the relatively high density of steel slag is fundamentally incompatible with the low bulk-density requirement of aerated concrete. Previous studies have shown that steel slag possesses a substantially higher density than conventional siliceous precursors such as fly ash, and increasing its replacement level generally reduces the expansion ratio, decreases pore volume, and increases the dry density of the hardened material [19]. Second, the mechanical improvements reported in many studies are often accompanied by increased material density and matrix densification. Consequently, it remains difficult to distinguish whether the observed strength enhancement originates from the intrinsic contribution of steel slag carbonation or simply from the increased density of the material [36, 51]. Therefore, although steel slag has been demonstrated to actively participate in carbonation reactions and improve certain engineering properties, existing studies have not fundamentally resolved the inherent conflict between achieving high steel slag utilization and maintaining the low bulk density required for high-performance aerated concrete.

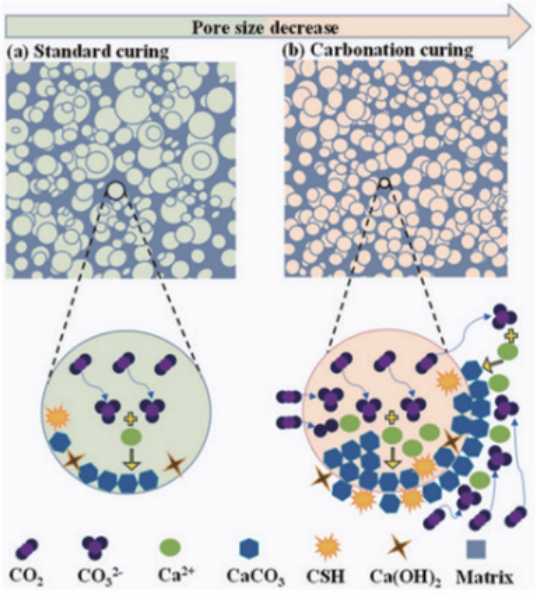
Regarding thermal performance, the thermal conductivity of CO_2 is lower than that of air, suggesting a potential improvement in thermal insulation during the initial stage. However, CO_2 within the pores may gradually be consumed by carbonation or escape and be replaced by air, potentially reducing this advantage over time. Meanwhile, carbonation can modify the pore structure through carbonate precipitation, thereby influencing heat transfer. Therefore, the long-term thermal performance of CO_2-aerated concrete depends on both pore structure and gas retention, which requires further investigation [52, 53].



(a) Standard curing



(b) Carbonation curing



(c) Microstructure development

Fig. 4. Air-void size distributions and CT-based 3D pore reconstructions of foamed concrete under (a) standard curing and (b) carbonation curing; (c) schematic illustration of microstructural development during carbonation[44].

2.4. Carbon sequestration

In CO_2-aerated concrete, carbon sequestration can be achieved through two pathways: chemical sequestration and physical sequestration. Chemical sequestration generally refers to the process by which CO_2 penetrates the pores of the material and reacts with unhydrated active constituents in the cement paste and their hydration products through carbonation, thereby generating stable solid products such as $CaCO_3$, Mg-based carbonates, and accompanying amorphous gels, which are immobilized within the material skeleton [14, 38, 50]. In contrast, physical carbon sequestration refers to the temporary storage of CO_2 within the material without mineralization, for instance as free gas in pores, dissolved CO_2/HCO^-_3 in the pore solution, or adsorbed CO_2 on pore walls. Fundamentally, this mechanism belongs to physical retention or adsorptive storage rather than chemical conversion [39, 45]. Existing studies indicate that carbon in concrete systems may occur either as solid carbonate minerals or as dissolved bicarbonate species [35, 54]. The former corresponds to chemical carbon sequestration, whereas the latter, together with pore adsorption, is more representative of physical carbon sequestration. Particularly in foamed concrete, carbonate minerals formed in situ on pore walls constitute the primary source of strength enhancement and long-term carbon sequestration, while adsorbed CO_2 or CO_2 stored in pores is generally considered a form of short-term retention or auxiliary carbon storage. Therefore, from the standpoint of long-term stable confinement, the principal carbon sequestration mechanism of CO_2-aerated concrete should still be regarded as chemically dominated sequestration, with physical sequestration playing a supplementary role. Table 1 summarizes the carbon sequestration capacities of CO_2-aerated concrete made with different raw materials.

Table 1. Carbon sequestration capacities of different CO_2-aerated concretes.

System	CO_2 Introduction Mode	Carbon Sequestration Mode	Indicator	Ref.
CAAC Based on Magnesium Slag	Curing	C	28 wt%	[41]
Pre-carbonated Red Mud Foamed Concrete	Curing	C	35.31 kg CO_2/m^3	[44]
MSW -ACB	Curing	C	23.4%	[47]
PC-Based CO_2 Foamed Concrete	Foam	C	61.0–85.7 kg CO_2/t	[43]

Note: All mass- and volume-normalized indicators are

expressed relative to concrete rather than cement. C: Chemical sequestration; P: Physical sequestration.

3. Carbon mineralization of steel slag

3.1. Characteristics and application challenges of steel slag

Steel slag is the solid byproduct generated during steel-making process [57]. On average, each ton of crude steel production is accompanied by approximately 0.1-0.15 tons of steel slag [24]. However, despite its massive production, the utilization rate of steel slag remains low. The primary disposal methods include stockpiling or landfilling, which not only occupy valuable land but also pose environmental risks due to the leaching of metal ions, potentially contaminating water and threatening human health.

The mineral composition of steel slag is similar to that of Portland cement, primarily consisting of tricalcium silicate (C_3S), dicalcium silicate (C_2S), RO phases (solid solutions containing magnesium, iron, and manganese oxides), and free lime (f-CaO) [25]. Considering the phase composition of steel slag and the need for large scale application , using steel slag as a building material is an ideal strategy for its resource utilization. However, steel slag faces two inherent limitations during application: it contains low content of C_3S, and high content of γ-C_2S, which exhibit poor hydraulic activity[58]. Consequently, the silicate phases in steel slag present slow hydration rates and poor early strength. Moreover, the volumes of f-CaO and free magnesium oxide (f-MgO) in steel slag will expand by 198% and 248%, respectively, upon hydration, leading to concrete cracking and decreasing the volume stability and durability of buildings.

This volume instability significantly constrains the large-scale, high-value utilization of steel slag. Therefore, effectively mitigating the potential expansion risks associated with f-CaO and f-MgO is essential for the efficient resource utilization of steel slag. Against this backdrop, CO_2 carbonation technology has emerged as a promising approach for steel slag treatment. It is well established that alkaline earth metal-rich mineral phases, particularly those containing Ca and Mg, can react with CO_2 to form thermodynamically stable carbonate minerals. This process not only reduces the volumetric expansion potential of steel slag but also enables the capture and permanent sequestration of CO_2. However, considerable debate remains within both the academic and engineering communities regarding the most effective form and strategy for incorporating carbonated steel slag into construction materials.

3.2. Carbonated steel slag as supplementary cementitious materials

The utilization of ground carbonated steel slag as a supplementary cementitious material (SCM) for partial cement replacement is one of the most extensively studied and applied methods. This method exhibits clear dual environmental benefits. First, during the carbonation stage, it directly consumes a certain amount of CO_2 [59]. Second, using carbonated steel slag powder as an SCM reduces the demand for Portland cement, thereby indirectly lowering the carbon emissions associated with cement production. Additionally, in the early stages of hydration, the fine calcium carbonate crystals generated during carbonation can act as nucleation sites, accelerating the precipitation of cement hydration products and thereby providing compensation for the early-age strength of the matrix.

Despite the aforementioned advantages, utilizing carbonated steel slag as SCM presents some inherent paradoxes. First, self-consumption of reactivity. The potential of steel slag as a cementitious material depends on its content of C_2S and C_3S. However, during the carbonation, CO_2 inevitably reacts not only with f-CaO but also with these hydraulic calcium silicates, converting them into non-hydraulic calcium carbonate and silica gel. Consequently, the higher the carbonation degree, the more stable the volume. However, this will result in a more severe loss of cementitious activity, and the final obtained powder will merely be an inert filler powder. Second, practical engineering constraints. Due to the loss of hydraulic activity, the replacement ratio of carbonated steel slag in concrete is typically limited to a low level (usually no more than 15-20%) [27, 28, 60]. As shown in Fig.5, exceeding this threshold whether in mortar or UHPC, often leads to a drastic decline in mechanical strength. Therefore, this low-volume application fails to satisfy the large- scale consumption requirement.

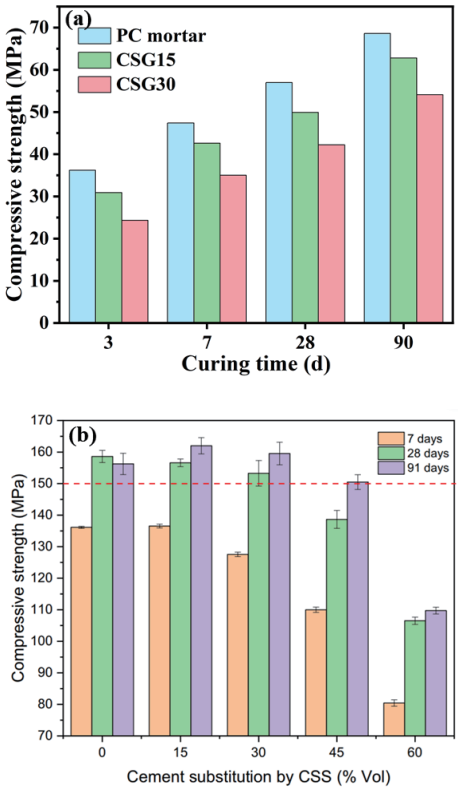


Fig.5. Influence of carbonated steel slag content on the compressive strength: (a) mortar samples [28]; (b) UHPC samples [60].

Table 2. Properties of carbonated steel slag and other aggregates [61].

Aggregates	Limestone	Coarse steel slag	Fine steel slag	waste glass	lightweight aggregate	Natural sand
Specific gravity	2.65	3.51	3.57	2.67	1.75	2.61
Dried density (kg/m^3)	2621	3174	3404	2668	1474	2611
Absorption (%)	0.32	2.95	1.31	NR	10.62	10.5

3.3. Carbonated steel slag as an aggregation

Another attractive application involves the use of carbonated crushed steel slag as an artificial aggregate [60]. Aggregates account for approximately 60% to 75% of the total volume of concrete, making the use of steel slag as aggregate one of the most direct and effective pathways for its large-scale utilization. During carbonation, f-CaO present on the surface of steel slag is rapidly converted into a dense calcium carbonate shell, thereby effectively reducing its volumetric instability. Furthermore, due to the inherently high density and hardness of steel slag, carbonated steel slag aggregates generally exhibit superior crushing resistance compared with natural aggregates. For example, Yu et al. [61] reported that replacing conventional coarse aggregates and natural sand with carbonated steel slag increased the density of concrete by 10% and 13%, respectively. A comparison of the properties of steel slag aggregates with those of other commonly used aggregates is presented in Table 2. Nevertheless, achieving a sufficient degree of carbonation is essential to reduce the contents of f-CaO and f-MgO to acceptable levels, thereby preventing deleterious expansion and ensuring the long-term dimensional stability of concrete.

Previous studies have developed a pathway from the direct use of carbonated steel slag to the production of artificial steel slag aggregates. Typically, steel slag aggregates are prepared by granulating steel slag powder, as shown in Fig.6(a). There are also studies on preparing carbonated steel slag aggregates by crushing carbonated steel slag compacts and then sieving (Fig.6(b)). Morone et al. [62] earlier demonstrated the application potential of artificial steel slag aggregates and investigated the relationship between granulation time and aggregates sizes. Pang et al. [63] demonstrated that carbonation could significantly enhance the strength and volume stability of artificial steel slag aggregates, while reducing water absorption rate and porosity. In addition, Jiang et al. [64] investigated the influence of two accelerated carbonation applied during granulation and curing on the characteristics of BOFS aggregates. Their results show that carbonation during granulation is inappropriate for producing high strength aggregates, but it is promising for producing lightweight aggregates.

On this basis, recent works have focused on optimizing the properties of artificial steel slag aggregates. For example, Mo et al. [66] enhanced the carbonation efficiency of steel slag aggregates through the incorporation of EDTA during the carbonation process. As illustrated in Fig. 7, concrete prepared with EDTA-modified carbonated steel slag aggregates exhibited compressive strengths that were 5.2–13.3 MPa higher than those of concrete containing carbonated aggregates produced without EDTA, demonstrating the effectiveness of EDTA in improving aggregate performance. In addition, Zhang et al. [67] used polycarboxylate superplasticizer as a strengthening additive. Moreover, Xu et al. [68] proposed a novel approach for preparing steel slag-based artificial lightweight aggregates by using biochar for internal carbonation. Although the aforementioned studies have further enhanced the performance of steel slag aggregates, these additional processing steps inevitably increase technical complexity and cost.

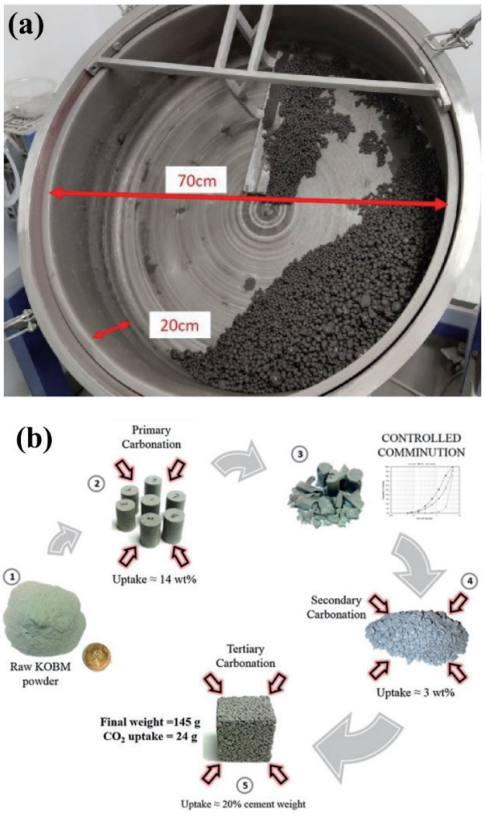


Fig. 6. Two methods for preparing carbonated steel slag aggregates [64]: (a) granulation; (b) crushing carbonated steel slag compacts [65].

At present, the practical application of carbonated steel slag

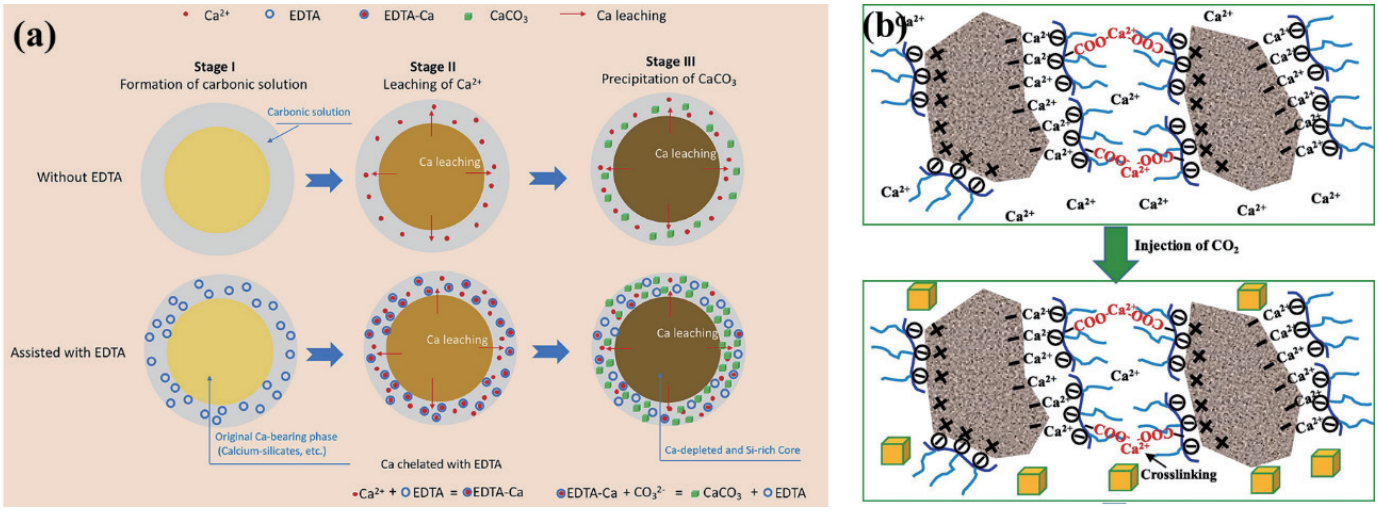


Fig. 7. Schematic diagram of the enhancement of steel slag aggregates by EDTA and PCE [66].

aggregates in concrete remains constrained by several significant challenges. First, controlling aggregate size and its influence on carbonation performance is essential. Aggregate size can be regulated by adjusting granulation time or through crushing and subsequent sieving[62–65]. Smaller aggregates generally exhibit higher carbonation efficiency due to their larger specific surface area and shorter CO_2 diffusion pathways. In contrast, larger aggregates are more likely to develop a dense $CaCO_3$ layer on the surface, which restricts further CO_2 penetration and leaves an incompletely carbonated core. Therefore, optimizing aggregate size and grading, together with carbonation conditions, is necessary to achieve sufficient carbonation while meeting practical requirements for concrete production. If such aggregates fracture during concrete mixing or under long-term service loading, the exposed internal f-CaO can subsequently react with water, resulting in localized expansive damage and compromising the long-term durability and service life of the structure. Second, although carbonated steel slag aggregates exhibit high intrinsic strength, their surfaces are typically coated with a relatively loose mixture of calcium carbonate and silica gel. As a result, when these aggregates are incorporated into cementitious matrices, the interfacial transition zone (ITZ) between the aggregate and cement paste often becomes the weakest region of the concrete, leading to a reduction in mechanical performance [69]. Finally, steel slag, which inherently possesses considerable cementitious potential, must be crushed through an energy-intensive process before being used merely as an inert aggregate. From both economic and resource-utilization perspectives, this approach fails to fully exploit the intrinsic value of steel slag and represents an inefficient use of the material.

3.4. Carbonated steel slag products

Based on the analysis of the aforementioned application pathways, it can be concluded that both the utilization of carbonated steel slag as a SCM or aggregate are finally constrained by the same challenge: how to safely incorporate an unstable material into another matrix. Therefore, by directly compacting the pure steel slag and then carbonating it, it can be directly produced into building materials, such as carbonized bricks, road bricks, slabs, etc., which is expected to be the best method for achieving its high-value utilization.

After proper pre-treatment, CO_2 can effectively diffuse into the inner regions of steel slag products [70]. The subsequent formation and precipitation of carbonates further fill pores and densify the microstructure [71, 72]. Previous studies have demonstrated that pure carbonated steel slag products possess sufficient mechanical performance. For instance, Xian et al. [73] demonstrated the feasibility of using steel slag as a 100% replacement for cement in concrete preparation (Fig.8(a)). After carbonation followed by water curing, the compressive strength of the steel slag compacts reaches 50 MPa. Humbert et al. [74] further improved the compressive strength of steel slag bricks to 70 MPa by optimizing the moisture content and compacting pressure [74] (Fig.8(b)). Ghouleh et al. [75] enhanced the reactivity of high-strength KOBM steel slag through carbonation, and their results showed that the resulting steel slag compacts reached a compressive strength of 80 MPa after only 2 h of carbonation. These studies indicate that carbonated steel slag products can achieve sufficient mechanical strength for use as building materials. More importantly, Zhang et al. [76] compared the mechanical performance and CO_2 capture capacity of fully steel slag-based bricks with those of fully carbide slag-based blocks. Their results revealed that steel slag blocks achieved a maximum carbonation degree of 24.56% and a compressive strength of 79.68 MPa. In contrast, carbide slag blocks exhibited a higher carbonation degree of 64.46% but a lower compressive strength of 44.64 MPa. These findings suggest that steel slag blocks can achive higher mechanical performance even under a relatively lower degree of carbonation. These products with the aforementioned strength are already sufficient for practical engineering applications. Moreover, Mahoutian et al. [77] further prepared pure steel slag bricks via carbonation and evaluated their freeze–thaw resistance against commercial

cement bricks. The commercial cement bricks started to lose mass after 2 cycles, while the steel slag bricks showed mass loss after 7 cycles. After 20 cycles, the mass loss of the commercial cement bricks reached 32%, compared with only 17% for the steel slag bricks. This means that the steel slag products not only possess satisfactory mechanical properties, but also exhibit excellent freeze-thaw resistance.

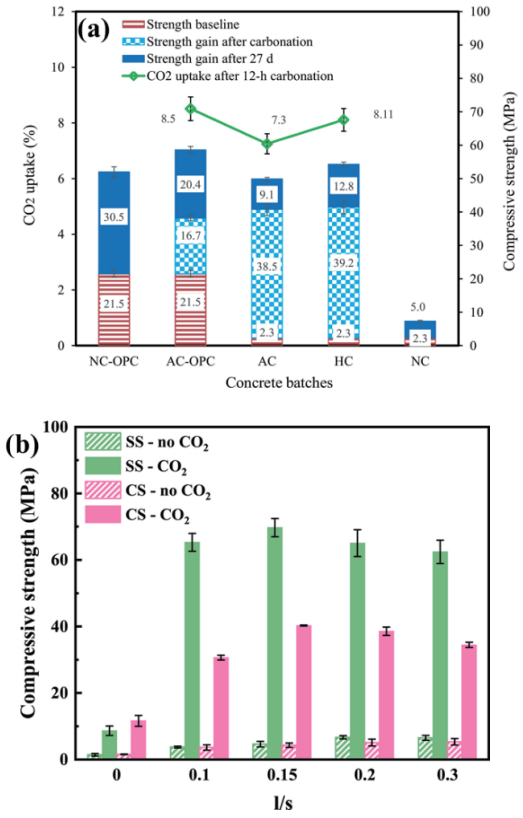


Fig.8. (a) the compressive strength of carbonated steel slag products [73]; (b) optimizing the moisture content to further enhance mechanical property [74].

Zhang et .al [78] reported that the GWP of 1 m^3 carbonated steel slag compacts was in the range of 39.2 to 247.5 kg CO_2-eq, which was much lower than 1204.4 kg CO_2-eq of conventional cured OPC. Moreover, the direct utilization of hot flue gas from the stack as the carbonation gas source can further decrease the GWP by 45%. For biochar-modified carbonated steel slag products, the lowest net CO_2 emission reached -39.9 kg/ton when the steel slag replacement ratio was 70% [79].

4. Influence of Al in aluminosilicate glass on its carbon mineralization

4.1. Basic structure of glassy phases and the function of Al

Aluminosilicate glass constitutes the principal reactive phase in many industrial by-products, including metallurgical slags and fly ash, and plays a decisive role in governing their CO_2 mineralization behavior. Consequently, understanding the structure of this amorphous phase and its influence on carbonation is essential for improving the carbon sequestration performance of these materials.

The glassy phase in alkaline industrial residues is composed predominantly of a three-dimensional framework of interconnected silicate tetrahedra ($[SiO_4]^{4-}$) linked through Si–O–Si bridging bonds. Network-modifying cations, such as alkali and alkaline-earth metals, partially disrupt this framework by breaking Si–O–Si linkages and generating non-bridging oxygen (NBO) sites, thereby increasing the chemical reactivity of the glass. Aluminum is generally incorporated as tetrahedrally coordinated $[AlO_4]^-$ units, which introduce a negative framework charge that must be compensated by alkali or alkaline-earth cations. Under conditions of insufficient charge compensation, aluminum may also occur in higher coordination states, including five- and six-coordinated species. Beyond the atomic scale, network formers and modifier cations are distributed heterogeneously, producing nanoscale compositional variations that influence dissolution behavior and ion transport during carbonation.

Recent investigations using both synthetic calcium aluminosilicate glasses and industrial by-products have demonstrated that aluminum controls carbonation through interconnected structural, transport, and interfacial mechanisms operating across multiple length scales. These studies have also identified key structural features that govern carbonation reactivity and provide potential pathways for enhancing CO_2 sequestration.

For example, Li et al. [29] examined the influence of Al_2O_3 on the carbonation behavior of synthetic calcium aluminosilicate ($CaO–Al_2O_3–SiO_2$) glasses, widely used as model systems for blast furnace slag and phosphorus slag. Their results showed that increasing the Al_2O_3 content progressively suppresses carbonation, leading to lower $CaCO_3$ formation and, under highly polymerized conditions, rendering the glass nearly inert to CO_2 mineralization when the non-bridging oxygen per tetrahedron (NBO/T) ratio decreases below 1.14. At the atomic level, aluminum was incorporated exclusively as tetrahedrally coordinated $[AlO_4]^-$ units, with Ca^{2+} ions serving as charge-balancing species. This substitution reduced the concentration of non-bridging oxygens, increased network polymerization, and restricted the mobility of Ca^{2+} ions required for carbonate precipitation. In addition to increasing network connectivity, the incorporation of aluminum promoted nanoscale phase separation, resulting in the formation of silicon-rich, calcium-depleted domains and highly polymerized regions dominated by $[AlO_4]^-$ and Q^4 silicate units. These heterogeneous structural domains disrupted the continuity of Ca^{2+} diffusion pathways, thereby reducing ion transport and slowing carbonation kinetics. Collectively, these findings demonstrate that aluminum exerts a dual inhibitory effect on CO_2 mineralization by simultaneously strengthening the glass network and impeding calcium diffusion, both of which limit the availability of reactive calcium for carbonate formation. Similar observations were reported by Yang et al. [30] in their investigation of phosphorus slag. Their study further revealed that phosphorus contributes to the formation of a more compact glass structure by promoting cross-linking between silicate chains, consistent with the highly amorphous characteristics identified

by X-ray diffraction analysis. The combined effects of aluminum and phosphorus induced network polymerization substantially reduce Ca^{2+} release during dissolution, thereby limiting the intrinsic carbonation reactivity of glass-rich industrial residues. These structural constraints provide a fundamental explanation for the persistent discrepancy between the theoretical CO_2 sequestration potential and the considerably lower carbonation capacities achieved experimentally in many industrial solid wastes.

4.2. Influence of Al on the carbonation behavior of synthetic glassy phases

The regulatory effect of Al on the glass network structure is directly reflected in its carbonation behavior. Compared with the Al-free binary $CaO–SiO_2$ glass, the degree of carbonation of the ternary $CaO–Al_2O_3–SiO_2$ glass is significantly reduced. As shown in Figs. 9 and 10, at a Ca/Si molar ratio of 1.0, the amount of calcium carbonate formed in the binary glass reached approximately 16 g per 100 g of raw material after 3 h of carbonation. Under the same conditions, however, the carbonation degree of the Al-containing ternary glass decreased markedly, and declined further with increasing Al content. Some high-Al samples exhibited almost no reactivity even after 48 h of carbonation [29, 31]. During carbonation, dissolved Ca^{2+} reacts with CO_3^{2-} to form $CaCO_3$, whereas Al and Si form a Ca-modified silica gel layer on the particle surface with the same stoichiometric ratio as in the original glass. Notably, zeta potential measurements showed that Al species preferentially adsorb onto the surface of glass particles. This competitive adsorption hinders the Ca^{2+} adsorption, thereby suppressing the heterogeneous nucleation of $CaCO_3$. SEM observations further confirmed that the $CaCO_3$ crystals precipitated on the $CaO–Al_2O_3–SiO_2$ glass were larger but exhibited a lower number density, in sharp contrast to the fine crystals that completely covered the surfaces of low-Al or Al-free glasses (see Fig. 11).

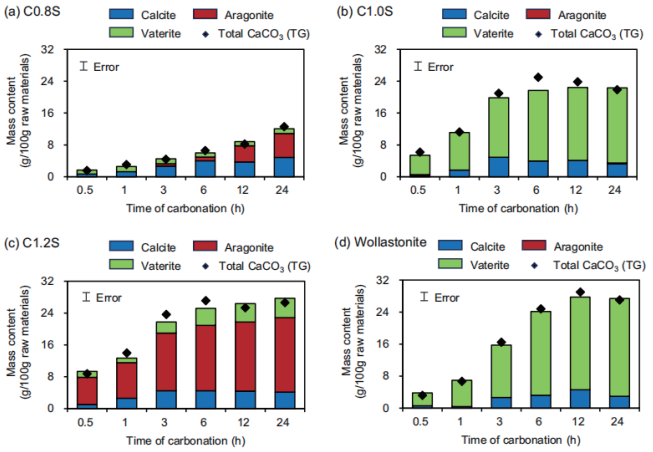


Fig. 9. Contents of different calcium carbonate polymorphs in the carbonated synthetic $CaO–SiO_2$ glass system [31].

4.3. Carbonation behavior of blast furnace slag

The influence of Al_2O_3 on the structure and reactivity of aluminosilicate glass is strongly dependent on the chemical

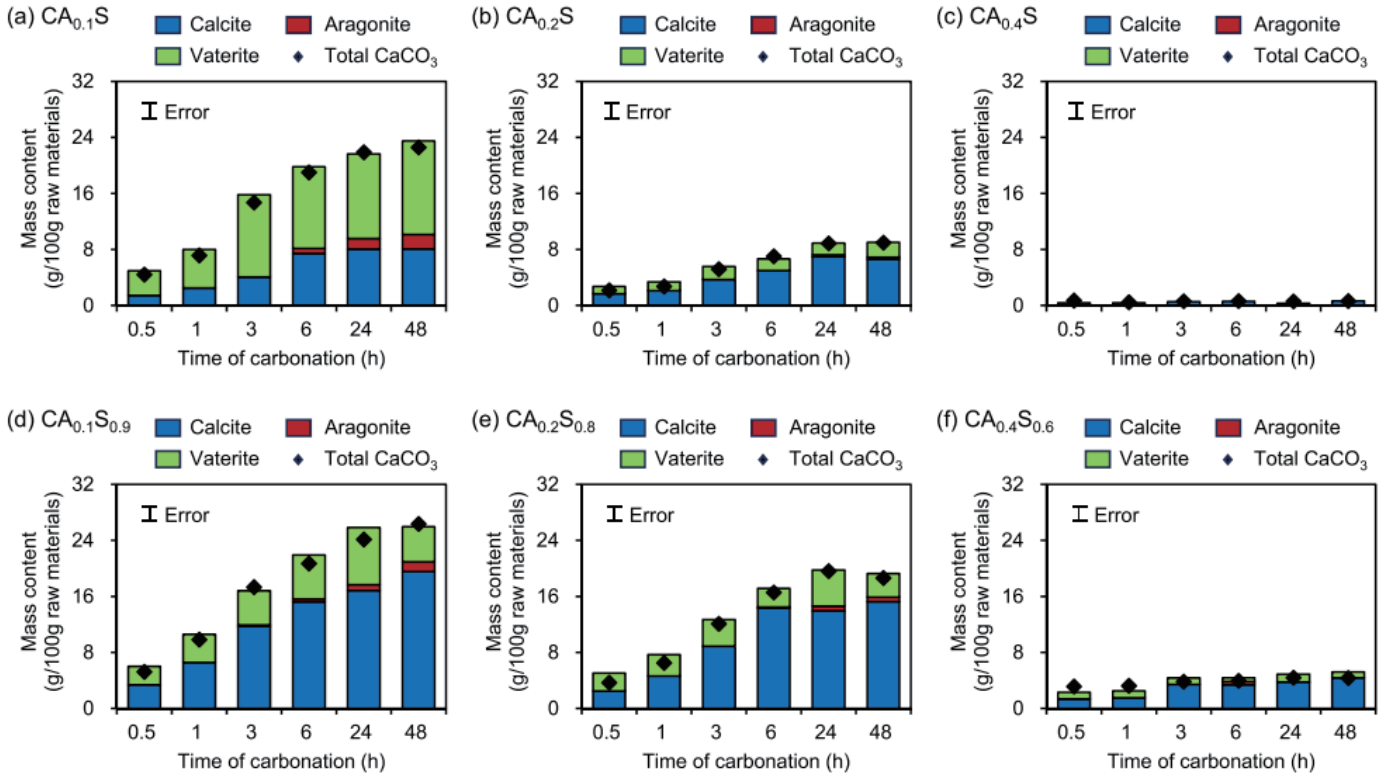


Fig. 10. Contents of different calcium carbonate polymorphs in the carbonated synthetic $CaO–Al_2O_3–SiO_2$ glass system [29].

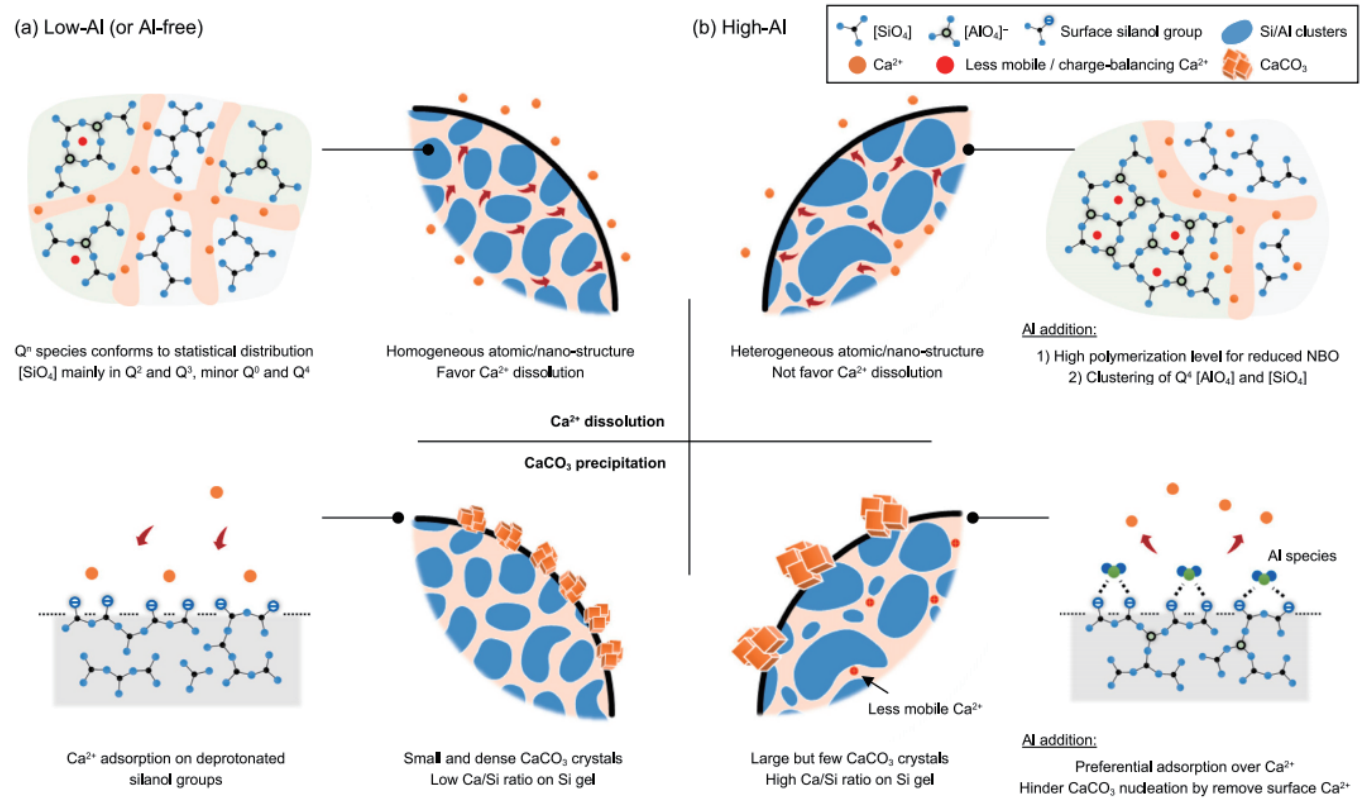


Fig. 11. Effect of Al on the atomic and nanoscale structure and carbonation behavior of CaO–Al_2O_3–SiO_2 Glasses: (a) Low-Al glass; (b) High-Al glass [29].

composition of the precursor. In percalcic (Ca-rich) glasses, such as blast furnace slag (BFS), the incorporation of Al_2O_3 modifies the glass network in a manner that generally increases its susceptibility to chemical dissolution. These structural changes enhance the pozzolanic reactivity of the glass by facilitating the release of reactive ionic species during the initial stages of dissolution [80]. However, this beneficial effect is often transient. As dissolution proceeds under alkaline conditions, dissolved aluminum species may adsorb onto the glass surface and subsequently reprecipitate, forming a passivating layer that suppresses further dissolution of the precursor [81, 82]. This surface passivation reduces the continued release of Ca^{2+} ions, which are essential for hydration and carbonation reactions. Consequently, the accumulation of aluminum-rich surface products can significantly retard reaction kinetics, particularly in alkali-activated and carbon mineralization systems where the availability of dissolved calcium governs carbonate precipitation.

Blast furnace slag, a representative calcium aluminosilicate glass, has been extensively studied to elucidate its carbonation behavior. As summarized in Table 3 and Fig. 12, the extent of direct carbonation remains limited over a wide range of curing durations and relative humidity conditions, with the carbonate content typically restricted to approximately 1–2 wt% [32, 33]. This low carbonation degree is primarily attributed to the inherent stability of the aluminosilicate glass network, which limits the dissolution of calcium and consequently constrains carbonate formation. In addition to the intrinsically slow dissolution kinetics, carbonation itself promotes the development of a surface passivation layer that further inhibits reaction progress. Xiang et al. [33] reported that dry carbonation produces a continuous $CaCO_3$ layer approximately 0.078–0.173μm thick on the slag surface (Table 4). This carbonating acts as a diffusion barrier, restricting the transport of CO_2 and dissolved ions to unreacted glass and thereby slowing subsequent carbonation. Collectively, these findings demonstrate that both the structural stability of the slag glass and the formation of protective surface layers are responsible for the limited carbonation efficiency of blast furnace slag.

Table 3. Carbonation product contents of slag under different carbonation times and humidity conditions [32].

Sample	S1	S2	35N65	3A65	7A65	3A95
Calcite (wt%)	0.3	0.2	0.3	0.2	0.2	0.2
Aragonite (wt%)	0	0.2	0.2	0.2	0.3	0.8
$CaCO_3$ (wt%)	0.3	0.4	0.5	0.4	0.5	1.0

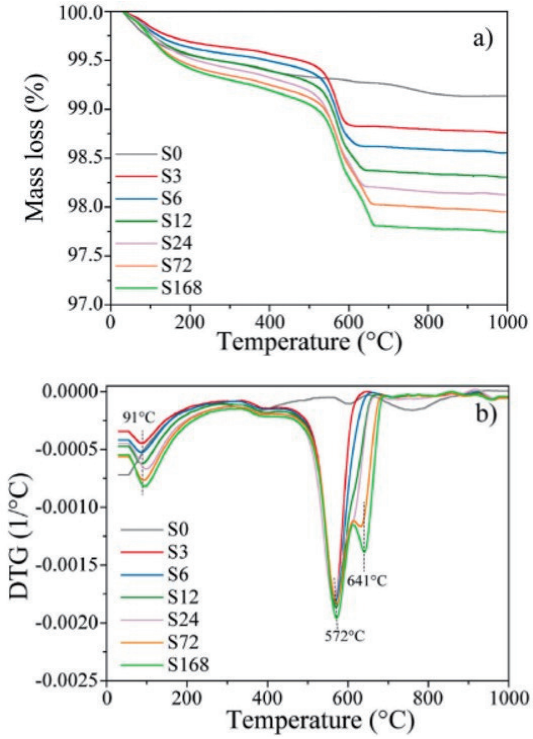


Fig. 12. TGA and DTG curves of slag carbonated for different periods [33].

Table 4. Thickness of the surface calcium carbonate layer on slag after different carbonation

Sample	S3	S6	S12	S24	S72	S168
Mass of Adsorbed CO_2 ($mgCO_2/g_{slag}$)	11.57	13.60	16.06	17.91	19.54	21.83
Thickness of the $CaCO_3$ layer (μm)	0.078	0.091	0.108	0.121	0.132	0.173

4.4. Carbonation behavior of fly ash

The incorporation of Al_2O_3 into $CaO–Al_2O_3–SiO_2$ glasses has been reported to depolymerize the aluminosilicate network of silica-rich (Si-rich) glasses, such as FA. This structural modification can enhance glass dissolution by increasing the susceptibility of the network to chemical attack. Nevertheless, compared with blast furnace slag, fly ash generally contains a higher alumina content and exhibits a more highly polymerized aluminosilicate glass network, which theoretically reduces its carbonation reactivity.

Despite this limitation, high-calcium fly ash still possesses considerable carbonation potential because of the presence of calcium-bearing phases, particularly free CaO. Cheng et al. [83] investigated the carbonation behavior of coal fly ash containing free CaO in seawater and found that the openness or closure of the reaction system had a significant effect on carbonation efficiency. At a liquid-to-solid ratio of 68 g/L, the carbonation efficiency of the open system reached 94.8%, whereas that of the sealed system was only 26.5%. They attributed this difference to the elevated CO_2 partial pressure (pCO_2) in the sealed system, which accelerated the formation of a $CaCO_3$ layer on the fly ash surface, thereby inhibiting the continued leaching of CaO from the particle interior. Furthermore, the cyclic carbonation method proposed in that study, whereby fresh fly ash and CO_2 were added in stages, increased the carbonation efficiency from 26.5% to 31.3%. Similarly, Lesmana et al. [84] found that calcium-bearing phases in fly ash, such as lime and anhydrite, reacted with carbonate ions (CO_3^{2-}) to form calcite. In that study, CO_2 was first absorbed by KOH to form a K_2CO_3 solution, thereby introducing carbonate ions (CO_3^{2-}) into the reaction system and effectively eliminating gas–liquid mass-transfer limitations. Consequently, the rate-controlling step of carbonation shifted to mineral dissolution. Collectively, these studies confirm the feasibility of carbon mineralization of calcium-bearing phases in fly ash. However, they do not elucidate the specific role of aluminum within the aluminosilicate glass network or its influence on the carbonation mechanism.

It should be noted that the influence of Al on carbonation depends not only on its content and structural environment but also on the composition of the precursor. In synthetic calcium aluminosilicate glasses, Al incorporation can inhibit carbonation by increasing glass network polymerization and restricting Ca^{2+} release[29]. However, in blast furnace slag and fly ash, carbonation behavior is also influenced by the availability of reactive calcium phases and the distribution of Al among different phases. Furthermore, the carbonation methods and conditions differ among these materials. The studies reviewed here involve gas–solid carbonation or pre-carbonation of blast furnace slag[32, 33] and aqueous carbonation of fly ash[83, 84], which differ from the CO_2 foaming and carbonation curing processes used for concrete products. These differences in material composition, moisture availability, CO_2 concentration, and mass transfer conditions should be considered when comparing carbonation performance. Therefore, the inhibitory effect of Al cannot be generalized across different material systems and carbonation conditions.

4.5. Improvement strategies

To address the limitation of carbonation reactivity caused by Al, researchers have explored a variety of enhancement strategies. Yang et al. [30] collectively demonstrated a wet grinding-assisted accelerated carbonation mechanism in which mechanical activation and chemical reactions act synergistically to enhance CO_2 sequestration in amorphous Ca–Si–Al–O glass systems. Their results show that intense shear and impact forces during wet grinding disrupt the highly

polymerized glass network, promoting cleavage of Si–O and Al–O bonds and driving progressive depolymerization of silicate species from Q^2/Q^3 units toward lower polymerized Q^1/Q^2 configurations. This transformation increases non-bridging oxygen (NBO) content, as confirmed by ^{29}Si MAS NMR, which reveals a pronounced rise in the Q^1 signal accompanied by a reduction in Q^2 and Q^3 species, indicating substantial network breakdown. This structural depolymerization significantly enhances Ca^{2+} mobility by weakening the binding strength within the aluminosilicate framework, leading to a marked increase in dissolved Ca^{2+} concentration (from 59.2 to 158 mg/L) and substantially improving carbonation efficiency. Consequently, CO_2 sequestration capacity reaches 131.9 kg/t slag, representing a 118% improvement over conventional bubbling carbonation (Fig. 13). Yan et al. [30] further clarified that this process proceeds through three coupled stages: (i) glass network depolymerization under mechanical stress, (ii) accelerated release of structurally bound Ca^{2+} into solution, and (iii) nucleation and precipitation of $CaCO_3$. In the final stage, $CaCO_3$ forms on particle surfaces; however, continuous grinding repeatedly removes the carbonate layer, exposing fresh reactive surfaces and establishing a cyclic "stripping–surface exposure–recarbonation" mechanism that sustains reactivity and enhances carbonation depth (Fig. 14). In addition, TEM observations reveal that mechanical action not only fractures the glass structure, generating microcracks and defect-rich regions, but also promotes continuous removal of passivating $CaCO_3$ layers. Grinding in a CO_2-rich environment further facilitates deformation-induced molecular mixing and accelerated diffusion along newly created boundaries, enabling partial incorporation of CO_2 into metastable carbonate species within silicate structures. Prolonged mechanical activation increases boundary density and surface area, thereby further enhancing CO_2 uptake. Overall, the study highlights that wet grinding intensifies both physical activation and chemical reactivity, enabling more efficient utilization of solid waste materials for accelerated mineral carbonation. Based on this principle, Matalkah and Soroushian [85] demonstrated that mechanical activation through ball milling enables effective incorporation of CO_2 into slag particles, resulting in enhanced reactivity and improved binding performance of alkali-activated geopolymer concrete. Their study showed that although CO_2-assisted milling has only a minor effect on particle size and morphology, it promotes mechanosorption of stable carbonate phases, predominantly amorphous or nanocrystalline in nature, on the slag surface, with occasional formation of crystalline carbonates such as dolomite. Importantly, the authors emphasized that the mechanical energy supplied during milling is essential for this process, as simple exposure of slag to CO_2 gas without milling does not achieve comparable carbonation or reactivity enhancement. During subsequent geopolymerization, these metastable carbonate phases participate in through-solution reactions, transforming into fine reaction products that become integrated within the developing aluminosilicate gel network. This integration strengthens the binder skeleton and contributes to a denser microstructure. As a result, significant improvements in mechanical performance were observed, with compressive strength increasing by up to 41% at early ages (1 day) compared to conventional air-milled slag systems. Overall, the findings of Matalkah et al. highlight the critical role of mechanochemical CO_2 activation in coupling carbonation with geopolymer chemistry to enhance the performance of alkali-activated materials.

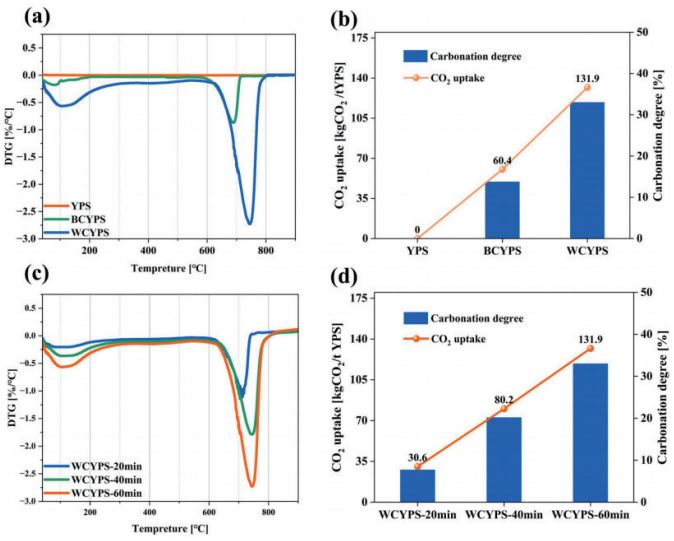


Fig. 13. Comparison of the carbonation efficiency of phosphorus slag under different treatment conditions: (a) DTG curves; (b) CO_2 uptake; (c) DTG analysis of WCYPS at different carbonation times; (d) carbonation efficiency of WCYPS at different reaction times [30]. (BCYPS: bubbling carbonation of phosphorus slag without wet grinding; WCYPS: wet grinding-driven accelerated carbonation of phosphorus slag; WYPS: wet-ground phosphorus slag without carbonation.)

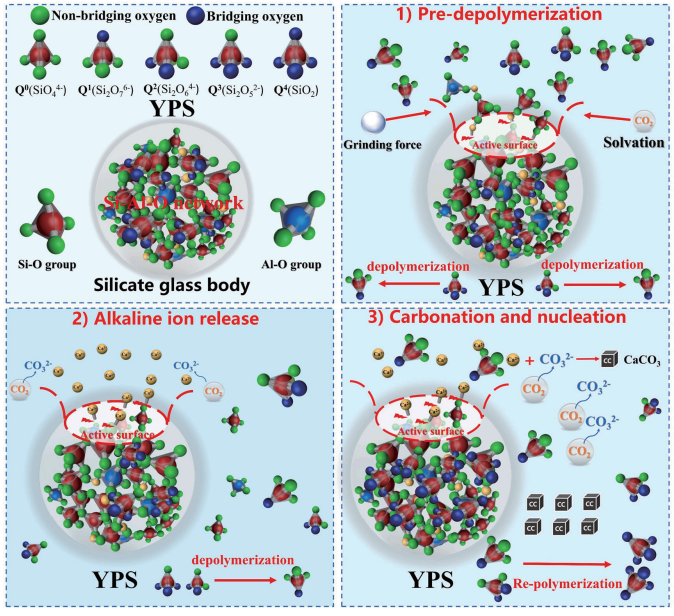


Fig. 14. Role of glassy network depolymerization in wet grinding-driven accelerated carbonation process [30].

5. Conclusion and perspectives

This review summarizes recent advances in CO_2-aerated concrete, the application of carbonated steel slag, and the role of aluminum in carbon mineralization. The main conclusions are as follows:

(1) CO_2-aerated concrete can be produced either by introducing CO_2 foam or by direct CO_2 curing. Both preparation methods exhibit an overall characteristic of synergistic development in lightweightness, thermal insulation, early-age strength, and carbon sequestration. From the perspective of long-term stable storage, the principal carbon sequestration mechanism in CO_2-aerated concrete should still be regarded as being dominated by chemical carbon sequestration. Future research should more rigorously distinguish between chemical and physical carbon sequestration, and establish a unified comparable accounting framework for carbon sequestration to accurately evaluate the actual carbon storage potential of these materials.

(2) Carbon-mineralized steel slag has been applied in various green building materials, such as supplementary cementitious materials, aggregates, and directly manufactured carbonated products, including blocks and bricks. The mechanical properties of products made solely from carbonated steel slag are sufficient to meet the requirements of practical engineering applications. In addition, the preparation process of steel slag bricks is simple and efficient, mainly involving crushing, mixing, pressing, and carbonation. At the same time, this route can also maximize CO_2 sequestration.

(3) The inhibitory effect of Al on carbonation can be understood at three levels. At the atomic scale, Al consumes non-bridging oxygen and disrupts Ca^{2+} transport pathways. At the nanoscale, Al induces phase separation and structural heterogeneity. During the reaction, Al adsorbs onto particle surfaces inhibiting $CaCO_3$ nucleation. This limitation may be alleviated through wet grinding or ball milling under a CO_2 atmosphere. Future research should focus on developing customized carbonation processes for different types of solid waste.

Despite the demonstrated feasibility of carbon mineralization in CO_2-aerated concrete, steel slag products, and aluminosilicate-based systems, several challenges must still be overcome before its broad industrial deployment:

(1) In CO_2-aerated concrete, carbon is stored as both chemically bound carbonates and physically retained CO_2. Because only the chemically fixed fraction provides long-term stable sequestration, future studies should clearly distinguish chemical carbon fixation from physical CO_2 retention and use consistent metrics and boundary conditions to ensure meaningful comparisons of reported carbon-storage capacities among different materials.

(2) Directly manufacturing fully carbonated steel slag products can avoid the compatibility issues and high grinding energy demand of the supplementary cementitious material route, as well as the ITZ associated with the aggregate route, while achieving excellent performance. Future studies should prioritize optimizating pretreatment, compaction, and carbonation parameters for large-scale components, the establishment of product standards and durability databases, and the validation of reliability and cost competitiveness in continuous pilot- and full-scale production lines.

(3) Although Al has been recognized to suppress carbonation across multiple scales, the unresolved mechanisms governing Al-mediated carbonation of real fly ash and slag glass phases remain to be elucidated.

Declaration of Competing Interest

There are no conflicts to declare.

Acknowledgements

The authors would like to acknowledge the financial support from National Natural Science Foundation of China grant numbers U22A20122 and 52678318, and Innovandi core project 10 of Global Cement and Concrete Association (GCCA).

References

[1] C. Shi, X. Hu, and Y. Mao, CO_2 Mineralization for Construction Materials and Products. CRC Press, 2026.

[2] Y. Mao, X. Hu, U. J. Alengaram, W. Chen, and C. Shi, "Use of carbonated recycled cement paste powder as a new supplementary cementitious material: A critical review," Cement and Concrete Composites, vol. 154, p. 105783, 2024/11/01/ 2024, doi: https://doi.org/10.1016/j.cemconcomp.2024.105783.

[3] Y. Mao, S. Drissi, P. He, X. Hu, J. Zhang, and C. Shi, "Quantifying the effects of wet carbonated recycled cement paste powder on the properties of cement paste," Cement and Concrete Research, vol. 175, p. 107381, 2024/01/01/ 2024, doi: https://doi.org/10.1016/j.cemconres.2023.107381.

[4] H. Mehdizadeh, S. Sarker, and M. Hajmohammadian Baghban, "Evaluating the efficacy of concrete washout water utilization in wet carbonation of hydrated cement waste considering temperature effects," Construction and Building Materials, vol. 482, p. 141688, 2025/07/04/ 2025, doi: https://doi.org/10.1016/j.conbuildmat.2025.141688.

[5] M. Wang, X. Hu, W. Chen, A. Khaskhoussi, S. Guo, and C. Shi, "Research on the carbonation hardening properties of fully recycled concrete powder compacts," Cement and Concrete Composites, vol. 170, p. 106556, 2026/07/01/ 2026, doi: https://doi.org/10.1016/j.cemconcomp.2026.106556.

[6] Y. Mao, P. He, S. Drissi, J. Zhang, X. Hu, and C. Shi, "Effect of conditions on wet carbonation products of recycled cement paste powder," Cement and Concrete Composites, vol. 144, p. 105307, 2023/11/01/ 2023, doi: https://doi.org/10.1016/j.cemconcomp.2023.105307.

[7] Y. Wang and C. Shi, "6 - Carbon dioxide sequestration on steel slag," in Carbon Dioxide Sequestration in Cementitious Construction Materials (Second Edition), F. Pacheco-Torgal, C. Shi, and A. Palomo Eds.: Woodhead Publishing, 2024, pp. 103-133.

[8] H.-J. Ho, A. Iizuka, E. Shibata, H. Tomita, K. Takano, and T. Endo, "CO_2 Utilization via Direct Aqueous Carbonation of Synthesized Concrete Fines under Atmospheric Pressure," ACS Omega, vol. 5, no. 26, pp. 15877-15890, 2020/07/07 2020, doi: 10.1021/acsomega.0c00985.

[9] Y. Jin, Z. Xiong, W. Feng, D. Zheng, S. Ng, and Y. Wang, "Semi-dry carbonated recycled concrete paste as alternative to limestone and its reactivity in LC3," Journal of Thermal Analysis and Calorimetry, vol. 149, no. 14, pp. 7215-7224, 2024/07/01 2024, doi: 10.1007/s10973-024-13266-6.

[10] W. K. Park, S.-J. Ko, S. W. Lee, K.-H. Cho, J.-W. Ahn, and C. Han, "Effects of magnesium chloride and organic additives on the synthesis of aragonite precipitated calcium carbonate," Journal of Crystal Growth, vol. 310, no. 10, pp. 2593-2601, 2008/05/01/ 2008, doi: https://doi.org/10.1016/j.jcrysgro.2008.01.023.

[11] H. Wang et al., "Enhanced reactivity of basic oxygen furnace slag by modified carbonation: Comparison among different calcium carbonate polymorphs," Cement and Concrete Composites, vol. 166, p. 106389, 2026/02/01/ 2026, doi: https://doi.org/10.1016/j.cemconcomp.2025.106389.

[12] J. Ye, S. Liu, J. Fang, H. Zhang, J. Zhu, and X. Guan, "Synthesis of Aragonite Whiskers by Co-Carbonation of Waste Magnesia Slag and Magnesium Sulfate: Enhancing Microstructure and Mechanical Properties of Portland Cement Paste," Buildings, vol. 13, no. 11, p. 2888doi: 10.3390/buildings13112888.

[13] C. Ramakrishna, T. Thenepalli, C. Han, and J.-W. Ahn, "Synthesis of aragonite-precipitated calcium carbonate from oyster shell waste via a carbonation process and its applications," Korean Journal of Chemical Engineering, vol. 34, no. 1, pp. 225-230, 2017/01/01 2017, doi: 10.1007/s11814-016-0264-6.

[14] J. Shao, S. Guo, and H. Wang, "A Review of the Performance, Sustainable Applications, and Research Challenges of Limestone-Calcined Clay-Cement (LC3) Systems," Coatings, vol. 15, no. 5, p. 611doi: 10.3390/coatings15050611.

[15] Y. Chen et al., "Can superabsorbent polymers be used as rheology modifiers for cementitious materials in the context of 3D concrete printing?," Construction and Building Materials, vol. 371, p. 130777, 2023/03/31/ 2023, doi: https://doi.org/10.1016/j.conbuildmat.2023.130777.

[16] Y. Zhao et al., "Development of reactive carbonate-calcined clay-cement (C4) composites through synchronizing aluminate-carbonate reaction: Toward high compressive strength and low carbon emission," Cement and Concrete Composites, vol. 160, p. 106060, 2025/07/01/ 2025, doi: https://doi.org/10.1016/j.cemconcomp.2025.106060.

[17] M. Lei, S. Deng, Z. Liu, F. Wang, and S. Hu, "Development of a Sustainable CO_2 Solidified Aerated Concrete," ACS Sustainable Chemistry & Engineering, vol. 10, no. 12, pp. 3990-4001, 2022/03/28 2022, doi: 10.1021/acssuschemeng.1c08695.

[18] T. Li, F. Huang, J. Zhu, J. Tang, and J. Liu, "Effect of foaming gas and cement type on the thermal conductivity of foamed concrete," Construction and Building Materials, vol. 231, p. 117197, 2020/01/20/ 2020, doi: https://doi.org/10.1016/j.conbuildmat.2019.117197.

[19] R. Sun et al., "Effects of curing regimes and binder designs on steel slag-based carbonated aerated concrete (CAC): Reaching a balance between pre-hydration and carbonation," Cement and Concrete Research, vol. 195, p. 107905, 2025/09/01/ 2025, doi: https://doi.org/10.1016/j.cemconres.2025.107905.

[20] I. Galan, F. P. Glasser, D. Baza, and C. Andrade, "Assessment of the protective effect of carbonation on portlandite crystals," Cement and Concrete Research, vol. 74, pp. 68-77, 2015/08/01/ 2015, doi: https://doi.org/10.1016/j.cemconres.2015.04.001.

[21] M. Zajac, I. Maruyama, A. Iizuka, and J. Skibsted, "Enforced carbonation of cementitious materials," Cement and Concrete Research, vol. 174, p. 107285, 2023/12/01/ 2023, doi: https://doi.org/10.1016/j.cemconres.2023.107285.

[22] Ö. Cizer, C. Rodriguez-Navarro, E. Ruiz-Agudo, J. Elsen, D. Van Gemert, and K. Van Balen, "Phase and morphology evolution of calcium carbonate precipitated by carbonation of hydrated lime," Journal of Materials Science, vol. 47, no. 16, pp. 6151-6165, 2012/08/01 2012, doi: 10.1007/s10853-012-6535-7.

[23] S. Zhang et al., "Influence mechanism of autoclaved aerated concrete waste on the hydration of blended cement with high-volume slag," Construction and Building Materials, vol. 447, p. 138180, 2024/10/11/ 2024, doi: https://doi.org/10.1016/j.conbuildmat.2024.138180.

[24] X. Liu, X. Liu, Z. Zhang, and X. Ai, "Effect of carbonation curing on the characterization and properties of steel slag-based cementitious materials," Cement and Concrete Composites, vol. 154, p. 105769, 2024/11/01/ 2024, doi: https://doi.org/10.1016/j.cemconcomp.2024.105769.

[25] Q. Dong, G. Wang, X. Chen, J. Tan, and X. Gu, "Recycling of steel slag aggregate in portland cement concrete: An overview," Journal of Cleaner Production, vol. 282, p. 124447, 2021/02/01/ 2021, doi: https://doi.org/10.1016/j.jclepro.2020.124447.

[26] Y. Wang, J. Liu, X. Hu, J. Chang, T. Zhang, and C. Shi, "Utilization of accelerated carbonation to enhance the application of steel slag: a review," Journal of Sustainable Cement-Based Materials, vol. 12, no. 4, pp. 471-486, 2023/04/03 2023, doi: 10.1080/21650373.2022.2154287.

[27] Y. Rui, C. Qian, X. Zhang, and Z. Ma, "Different carbon treatments for steel slag powder and their subsequent effects on properties of cement-based materials," Journal of Cleaner Production, vol. 362, p. 132407, 2022/08/15/ 2022, doi: https://doi.org/10.1016/j.jclepro.2022.132407.

[28] P. Liu, J. Zhong, M. Zhang, L. Mo, and M. Deng, "Effect of CO2 treatment on the microstructure and properties of steel slag supplementary cementitous materials," Construction and Building Materials, vol. 309, p. 125171, 2021/11/22/ 2021, doi: https://doi.org/10.1016/j.conbuildmat.2021.125171.

[29] C. Li et al., "Effect of alumina on the carbonation reactivity of calcium aluminosilicate glasses," Cement and Concrete Research, vol. 199, p. 108023, 2026/01/01/ 2026, doi: https://doi.org/10.1016/j.cemconres.2025.108023.

[30] J. Yang et al., "Accelerated aqueous carbonation of phosphorous slag driven by grinding force: The role of depolymerization of glassy network," Chemical Engineering Journal, vol. 524, p. 169432, 2025/11/15/ 2025, doi: https://doi.org/10.1016/j.cej.2025.169432.

[31] C. Li et al., "Carbonation reactivity of calcium silicate glasses at various calcium to silicate ratios and comparison with wollastonite," Cement and Concrete Research, vol. 186, p. 107653, 2024/12/01/ 2024, doi: https://doi.org/10.1016/j.cemconres.2024.107653.

[32] M. Mutti, S. Joseph, R. Snellings, and Ö. Cizer, "Effect of slag pre-carbonation on its early-age reactivity in alkali activated binder," Construction and Building Materials, vol. 411, p. 134413, 2024/01/12/ 2024, doi: https://doi.org/10.1016/j.conbuildmat.2023.134413.

[33] J. Xiang, Y. He, X. Cui, and L. Liu, "Enhancement of setting times and hardening of alkali-activated slag binder using CO2-modified slag," Cement and Concrete Composites, vol. 134, p. 104797, 2022/11/01/ 2022, doi: https://doi.org/10.1016/

j.cemconcomp.2022.104797.
[34] Z. Wang et al., "Unveiling the role of reactive magnesia and red mud in CO_2-cured aerated concrete," Journal of Building Engineering, vol. 78, p. 107704, 2023/11/01/ 2023, doi: https://doi.org/10.1016/j.jobe.2023.107704.
[35] R. Zheng, J. Xia, E. Liu, Q. Zhou, and H. Wang, "A high water-cement ratio aerated concrete using carbon dioxide as the foaming agent: Mix design, pore structure and hydration products," Journal of Building Engineering, vol. 108, p. 112926, 2025/08/15/ 2025, doi: https://doi.org/10.1016/j.jobe.2025.112926.
[36] J. Chen et al., "Synergistic enhancement mechanism of hydration and carbonation and performance optimization for steel slag-cement foam concrete: Regulatory role of CO2 injection mixing process," Construction and Building Materials, vol. 513, p. 145195, 2026/02/28/ 2026, doi: https://doi.org/10.1016/j.conbuildmat.2026.145195.
[37] L. Jiang, Z. Wang, Y. Wang, J. Niu, and J. Qin, "Preparation and properties of carbon dioxide foamed concrete using nanoparticles as foam stabilizer and pre–carbonated cement slurry," Cement and Concrete Composites, vol. 151, p. 105585, 2024/08/01/ 2024, doi: https://doi.org/10.1016/j.cemconcomp.2024.105585.
[38] D. Fan, J.-X. Lu, X.-S. Lv, T. Noguchi, R. Yu, and C. S. Poon, "Carbon capture and storage CO_2 foam concrete towards higher performance: Design, preparation and characteristics," Cement and Concrete Composites, vol. 157, p. 105925, 2025/03/01/ 2025, doi: https://doi.org/10.1016/j.cemconcomp.2025.105925.
[39] X. Ta, Y. Zhang, Z. Wan, P. Shi, and J. Zhou, "Study on Preparation and Performance of CO_2 Foamed Concrete for Heat Insulation and Carbon Storage," Materials, vol. 16, no. 7, p. 2725doi: 10.3390/ma16072725.
[40] L. Jiang, Z. Wang, Y. Wang, and J. Niu, "Improvement of calcium sulfoaluminate foamed concrete by carbon dioxide foam: hydration activation and pore structure optimization," Cement and Concrete Composites, vol. 163, p. 106162, 2025/10/01/ 2025, doi: https://doi.org/10.1016/j.cemconcomp.2025.106162.
[41] M. Lei, S. Deng, K. Huang, Z. Liu, F. Wang, and S. Hu, "Preparation and characterization of a CO_2 activated aerated concrete with magnesium slag as carbonatable binder," Construction and Building Materials, vol. 353, p. 129112, 2022/10/24/ 2022, doi: https://doi.org/10.1016/j.conbuildmat.2022.129112.
[42] X. Ta, Y. Zhang, Z. Wan, and J. Li, "Study on preparation method and carbon fixation performance of supercritical CO^2-foamed concrete," Construction and Building Materials, vol. 491, p. 142759, 2025/09/12/ 2025, doi: https://doi.org/10.1016/j.conbuildmat.2025.142759.
[43] X. Ta, Z. Wan, Y. Zhang, S. Qin, and J. Zhou, "Effect of carbonation and foam content on CO_2 foamed concrete behavior," Journal of Materials Research and Technology, vol. 23, pp. 6014-6022, 2023/03/01/ 2023, doi: https://doi.org/10.1016/j.jmrt.2023.02.178.
[44] Q. Liu, Y. Wang, C. Sun, S. Cheng, and C. Yang, "Carbon sequestration and mechanical properties of foam concrete based on red mud pre-carbonation and CO_2 foam bubbles," Construction and Building Materials, vol. 426, p. 135961, 2024/05/03/ 2024, doi: https://doi.org/10.1016/j.conbuildmat.2024.135961.
[45] X. Wei, J. Li, H. Shi, Y. Cao, and G. Liu, "Experimental study on CO_2 sequestration performance of alkali activated fly ash and ground granulated blast furnace slag based foam concrete," Construction and Building Materials, vol. 447, p. 138043, 2024/10/11/ 2024, doi: https://doi.org/10.1016/j.conbuildmat.2024.138043.
[46] J. Lu, X. Diao, Q. Zeng, D. Yan, Y. Song, and T. Shi, "Multiscale elucidation of porosity as a regulatory factor in CO_2 curing of aerated cement based materials," Journal of Building Engineering, vol. 120, p. 115493, 2026/02/15/ 2026, doi: https://doi.org/10.1016/j.jobe.2026.115493.
[47] Y. Sun et al., "Aerated concrete made of MSW incineration ash: Effect of blending materials and CO_2 curing condition," Journal of Environmental Chemical Engineering, vol. 12, no. 6, p. 114715, 2024/12/01/ 2024, doi: https://doi.org/10.1016/j.jece.2024.114715.
[48] Y.-L. Liu, C.-F. Li, H.-X. Zhai, M. Riaz Ahmad, D. Guo, and J.-G. Dai, "Production and performance of CO_2 modified foam concrete," Construction and Building Materials, vol. 389, p. 131671, 2023/07/31/ 2023, doi: https://doi.org/10.1016/j.conbuildmat.2023.131671.
[49] M. Lei, S. Deng, Z. Liu, F. Wang, and S. Hu, "Understanding of EPS beads on mechanical properties and void morphology of a CO_2-solidified foam concrete based on solid wastes," Construction and Building Materials, vol. 405, p. 133388, 2023/11/17/ 2023, doi: https://doi.org/10.1016/j.conbuildmat.2023.133388.
[50] D. Yan et al., "CO_2 Pretreatment to Aerated Concrete with High-Volume Industry Wastes Enables a Sustainable Precast Concrete Industry," ACS Sustainable Chemistry & Engineering, vol. 9, no. 8, pp. 3363-3375, 2021/03/01 2021, doi: 10.1021/acssuschemeng.1c00001.
[51] X. Gu et al., "Improving physical properties, microstructure and actual carbon sequestration of steel slag based autoclaved aerated concrete by accelerated carbonation," Journal of Building Engineering, vol. 94, p. 110045, 2024/10/01/ 2024, doi: https://doi.org/10.1016/j.jobe.2024.110045.
[52] C. Wen et al., "Study of macro-/micro-properties and in-situ mineralization mechanism of CO_2 foam concrete based on solid waste-derived SAC-gypsum composite," Construction and Building Materials, vol. 486, p. 141911, 2025/08/08/ 2025, doi: https://doi.org/10.1016/j.conbuildmat.2025.141911.
[53] T. Li, F. Huang, L. Li, J. Zhu, X. Jiang, and Y. Huang, "Preparation and properties of sulphoaluminate cement-based foamed concrete with high performance," Construction and Building Materials, vol. 263, p. 120945, 2020/12/10/ 2020, doi: https://doi.org/10.1016/j.conbuildmat.2020.120945.
[54] S. Yao et al., "Development of an Aerated Sulfoaluminate Cement–Based Material for Coal Mine Filling," Journal of Materials in Civil Engineering, vol. 35, no. 2, p. 04022436, 2023/02/01 2023, doi: 10.1061/(ASCE)MT.1943-5533.0004608.
[55] J. Zhang, Y. Su, and H. Gao, "Development of CO_2-ceramsite foam concrete: Mechanical properties, microstructure and environmental benefits," Case Studies in Construction Materials, vol. 23, p. e04957, 2025/12/01/ 2025, doi: https://doi.org/10.1016/j.cscm.2025.e04957.
[56] L. Han, X. Wang, B. Wu, S. Zhu, J. Wang, and Y. Zhang, "In-situ synthesis of zeolite X in foam geopolymer as a CO_2 adsorbent," Journal of Cleaner Production, vol. 372, p. 133591, 2022/10/20/ 2022, doi: https://doi.org/10.1016/j.jclepro.2022.133591.
[57] C. Shi, "Characteristics and cementitious properties of ladle slag fines from steel production," Cem. Concr. Res., vol. 32,

pp. 459-462, 2002.
[58] M. Zhu, Q. Yu, S. R. Laan, Y. Chen, " Dipotassium hydrogen phosphate activated Al-rich steel slag: The role of layered double hydroxides and aluminum hydrate gel," Cem. Concr. Res., vol. 189, pp. 107783, 2025, doi: 10.1016/j.cemconres.2025.107783.
[59] Jyoti, B. Pal, and S. K. Singh, "Degree of reactivity and strength evolution of ground steel slag-based composite binder – experimental and numerical analysis," Journal of Sustainable Cement-Based Materials, vol. 15, no. 5, pp. 1627-1645, 2026/05/04 2026, doi: 10.1080/21650373.2025.2611405.
[60] G. Liu, K. Schollbach, P. Li, and H. J. H. Brouwers, "Valorization of converter steel slag into eco-friendly ultra-high performance concrete by ambient CO_2 pre-treatment," Construction and Building Materials, vol. 280, p. 122580, 2021/04/19/ 2021, doi: https://doi.org/10.1016/j.conbuildmat.2021.122580.
[61] X. Yu, Z. Tao, T.-Y. Song, and Z. Pan, "Performance of concrete made with steel slag and waste glass," Constr. Build. Mater., vol. 114, pp. 737-746, 2016, doi: 10.1016/j.conbuildmat.2016.03.217.
[62] M. Morone, G. Costa, A. Polettini, R. Pomi, and R. Baciocchi, "Valorization of steel slag by a combined carbonation and granulation treatment," Miner. Eng., vol. 59, pp. 82-90, 2014, doi: 10.1016/j.mineng.2013.08.009.
[63] B. Pang, Z. Zhou, and H. Xu, "Utilization of carbonated and granulated steel slag aggregate in concrete," Constr. Build. Mater., vol. 84, pp. 454-467, 2015, doi: 10.1016/j.conbuildmat.2015.03.008.
[64] Y. Jiang and T.-C. Ling, "Production of artificial aggregates from steel-making slag: Influences of accelerated carbonation during granulation and/or post-curing," J. CO_2 Util., vol. 36, pp. 135-144, 2020, doi: 10.1016/j.jcou.2019.11.009.
[65] Z. Ghouleh, R. I. L. Guthrie, and Y. Shao, "Production of carbonate aggregates using steel slag and carbon dioxide for carbon-negative concrete," J. CO_2 Util., vol. 18, pp. 125-138, 2017, doi: 10.1016/j.jcou.2017.01.009.
[66] S. Yang, L. Mo, and M. Deng, "Effects of ethylenediamine tetra-acetic acid (EDTA) on the accelerated carbonation and properties of artificial steel slag aggregates," Cement and Concrete Composites, vol. 118, p. 103948, 2021/04/01/ 2021, doi: https://doi.org/10.1016/j.cemconcomp.2021.103948.
[67] Y. Zhang, M. Zhang, and D. Huang, "Polycarboxylate superplasticizer as strengthening additive in carbonated artificial steel slag aggregate," Constr. Build. Mater., vol. 403, p. 133136, 2023, doi: 10.1016/j.conbuildmat.2023.133136.
[68] M. Xu, Y. Zhang, S. Yang, L. Mo, and P. Liu, "Effects of internal CO_2 curing provided by biochar on the carbonation and properties of steel slag-based artificial lightweight aggregates (SALAs)," Cement and Concrete Composites, vol. 142, p. 105197, 2023/09/01/ 2023, doi: https://doi.org/10.1016/j.cemconcomp.2023.105197.
[69] M. E. Mitwally, A. Elnemr, A. Shash, and A. Babiker, "Utilization of steel slag as partial replacement for coarse aggregate in concrete," Innovative Infrastructure Solutions, vol. 9, no. 5, 2024, doi: 10.1007/s41062-024-01464-y.
[70] C. Shi, F. He, and Y. Wu, "Effect of pre-conditioning on CO_2 curing of lightweight concrete blocks mixtures," Constr. Build. Mater., vol. 26, no. 1, pp. 257-267, 2012, doi: 10.1016/j.conbuildmat.2011.06.020.
[71] B. Lu, C. Shi, and G. Hou, "Strength and microstructure of CO_2 cured low-calcium clinker," Constr. Build. Mater., vol. 188, pp. 417-423, 2018, doi: 10.1016/j.conbuildmat.2018.08.134.
[72] B. Lu, C. Shi, Z. Cao, M. Guo, and J. Zheng, "Effect of carbonated coarse recycled concrete aggregate on the properties and microstructure of recycled concrete," J. Cleaner Prod., vol. 233, pp. 421-428, 2019, doi: 10.1016/j.jclepro.2019.05.350.
[73] X. Xian, M. Mahoutian, D. Zhang, and Y. Shao, "Development of wet-cast Portland-cement-free concrete based on steel slag and ambient-pressure carbonation activation," Resour. Conserv. Recycl., vol. 203, p. 107455, 2024, doi: 10.1016/j.resconrec.2024.107455.
[74] P. S. Humbert, J. P. Castro-Gomes, and H. Savastano, "Clinker-free CO_2 cured steel slag based binder: Optimal conditions and potential applications," Constr. Build. Mater., vol. 210, pp. 413-421, 2019, doi: 10.1016/j.conbuildmat.2019.03.169.
[75] Z. Ghouleh, R. I. L. Guthrie, and Y. Shao, "High-strength KOBM steel slag binder activated by carbonation," Constr. Build. Mater., vol. 99, pp. 175-183, 2015, doi: 10.1016/j.conbuildmat.2015.09.028.
[76] Q. Zhang, P. Feng, X. Shen, Y. Cai, H. Zhen, and Z. Liu, "Comparative analysis of carbonation strengthening mechanisms in full solid waste materials: Steel slag vs. carbide slag," Cement and Concrete Composites, vol. 157, p. 105927, 2025/03/01/ 2025, doi: https://doi.org/10.1016/j.cemconcomp.2025.105927.
[77] M. Mahoutian and Y. Shao, "Production of cement-free construction blocks from industry wastes," J. Cleaner Prod., vol. 137, pp. 1339-1346, 2016, doi: 10.1016/j.jclepro.2016.08.012.
[78] S. Zhang, Z. Ghouleh, J. Liu, and Y. Shao, "Converting ladle slag into high-strength cementing material by flue gas carbonation at different temperatures," Resources, Conservation and Recycling, vol. 174, p. 105819, 2021/11/01/ 2021, doi: https://doi.org/10.1016/j.resconrec.2021.105819.
[79] J. Liu et al., "Carbonation of steel slag at low CO2 concentrations: Novel biochar cold-bonded steel slag artificial aggregates," Sci. Total Environ., vol. 902, p. 166065, 2023, doi: 10.1016/j.scitotenv.2023.166065.
[80] S. Kucharczyk et al., "Structure and reactivity of synthetic CaO-Al_2O_3-SiO_2 glasses," Cement and Concrete Research, vol. 120, pp. 77-91, 2019/06/01/ 2019, doi: https://doi.org/10.1016/j.cemconres.2019.03.004.
[81] R. Snellings, "Solution-Controlled Dissolution of Supplementary Cementitious Material Glasses at pH 13: The Effect of Solution Composition on Glass Dissolution Rates," Journal of the American Ceramic Society, vol. 96, no. 8, pp. 2467-2475, 2013/08/01 2013, doi: https://doi.org/10.1111/jace.12480.
[82] K. C. Newlands, M. Foss, T. Matchei, J. Skibsted, and D. E. Macphee, "Early stage dissolution characteristics of aluminosilicate glasses with blast furnace slag- and fly-ash-like compositions," Journal of the American Ceramic Society, vol. 100, no. 5, pp. 1941-1955, 2017/05/01 2017, doi: https://doi.org/10.1111/jace.14716.
[83] T. Cheng et al., "Cyclic aqueous carbonation of fly ash in seawater: Enhancing carbonation efficiency and CO_2 removal rate," Chemical Engineering and Processing - Process Intensification, vol. 216, p. 110428, 2025/10/01/ 2025, doi: https://doi.org/10.1016/j.cep.2025.110428.
[84] M. J. Lesmana, T. Nozaki, X. Fan, A. Darmawan, and F. B. Juangsa, "Utilization of fly ash for CO_2 capture through mineral carbonation: An experimental study with Indonesian

coal fly ash," Chinese Journal of Chemical Engineering, vol. 91, pp. 255-265, 2026/03/01/ 2026, doi: https://doi.org/10.1016/j.cjche.2025.10.025.

[85] F. Matalkah and P. Soroushian, "CO_2 treatment of ground granulated blast furnace slag for enhancing geopolymer properties," Journal of Materials Research and Technology, vol. 17, pp. 2457-2465, 2022/03/01/ 2022, doi: https://doi.org/10.1016/j.jmrt.2022.01.161.

[86] F. Xie et al., "Surface chemistry controlled carbonation of amorphous calcium (alumino) silicate slags in aqueous solutions," Construction and Building Materials, vol. 506, p. 144930, 2026/01/13/ 2026, doi: https://doi.org/10.1016/j.conbuildmat.2025.144930.